Electronic Supplementary Material (ESI) for Journal of Materials Chemistry A.

Supporting Information

Multifunctional Ultrathin Aluminum Foil: Oil/Water Separation and Particle Filtration

Guoqiang Li,[a] Hua Fan,[b] Feifei Ren,[c] Chen Zhou,[d] Zhen Zhang,[a] Bing Xu,[a] Sizhu Wu,[d] Yanlei Hu,[a] Wulin Zhu,[a] Yishan Zeng,[b] Xiaohong Li,[e] Jiaru Chu,[a] and Dong Wu*[a]*

[a] CAS Key Laboratory of Mechanical Behavior and Design of Materials, Department of Precision Machinery and Precision Instrumentation, University of Science and Technology of China, Hefei, Anhui, 230026, P. R. China.
[b] Department of Mechanical and Electronic Engineering, Hefei University of Technology, Hefei, Anhui, 230009, P. R. China.
[c] School of Electrical Engineering and Automation, Anhui University, Hefei, Anhui, 230601, P. R. China.
[d] School of Instrument Science and Opto-electronics Engineering, Hefei University of Technology, Hefei, Anhui, 230009, P. R. China.
[e] Joint Laboratory for Extreme Conditions Matter Properties, School of Science, Southwest University of Science and Technology, Mianyang, Sichuan, 621010, China.
*E-mail: huyl@ustc.edu.cn and dongwu@ustc.edu.cn

Keywords: (Ultrathin aluminum foil; Micropore arrays; Oil/water separation; Particle filtration)

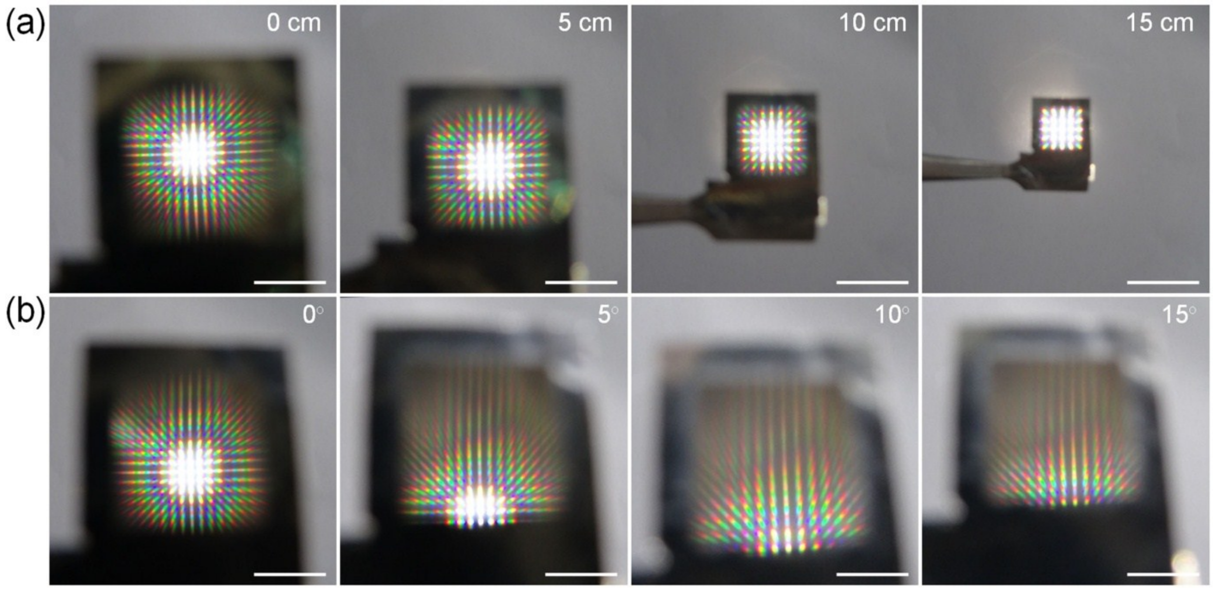

Figure S1. Bright iridescence formed by the regular micropore arrays due to the optical diffraction effect. (a) The four iridescent patterns taken by different distance from the foils to the camera. The distances are 0, 5, 10, 15 cm, respectively. (b) The iridescent patterns taken by different angles to the optical axis, and the included angles are 0°, 5°, 10°, and 15°, respectively. All the samples are irradiated by white LED from the behind.

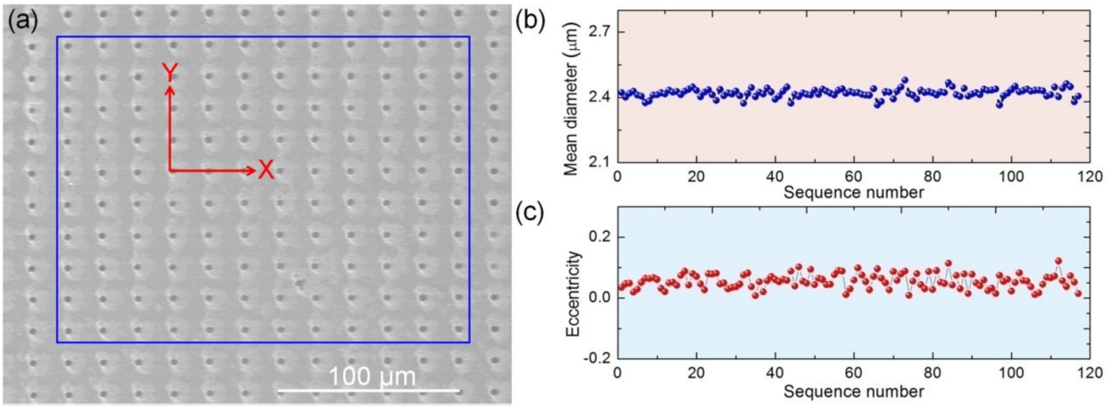

Figure S2. Uniformity analysis of the micropores formed by femtosecond laser perforating. (a) is the SEM image of the micropore arrays. The interval of the adjacent pores is 20 μm. (b) is the mean diameter of the pores by averaging the X and Y directions in the blue area in (a). (c) is the analysis of the eccentricity of the each pore in the blue area in (a). It can be seen that all the eccentricity is less than 0.1, which means that the pores are very equivalent to roundness. From (b) and (c), it is indicated that regular micropores are arrayed on the aluminum foil surface.

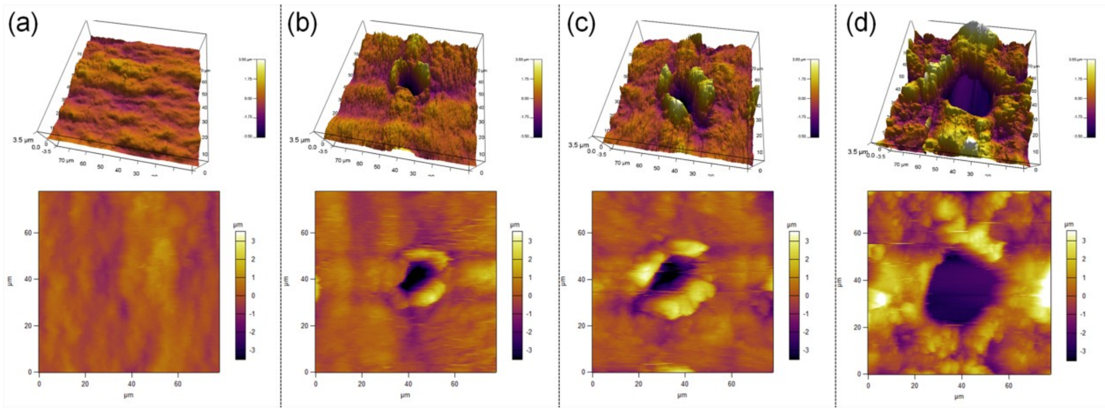

Figure S3. The measurement of the surface roughness of the aluminum foil. (a) The untreated aluminum foil and the surface roughness is ~372.6 nm. (b) The femtosecond laser processed aluminum foil with pore diameter of ~ 8.9 μm, and the surface roughness is ~709.9 nm. (c) The aluminum foil with pore size of ~ 14.6 μm, and the roughness is ~864.7 nm. (d) The aluminum foil with pore size of ~ 24.8 μm, and the roughness is ~1393 nm.

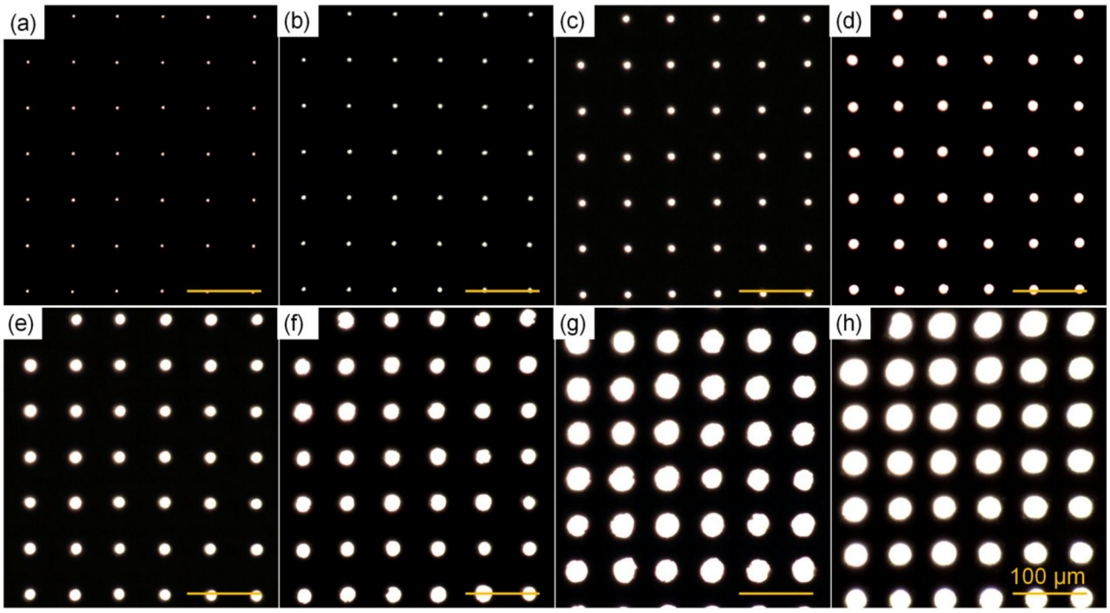

Figure S4. Optical microscope images of the micropores. From (a) to (h), the diameters are 2.4, 4.1, 8.2, 12.2, 15.9, 19.1, 27.7, and 32.2 μm, respectively. The results indicate that not only the pores are uniformly distributed, but also the micropores can be tuned by changing the laser pulse energy and pulse numbers.

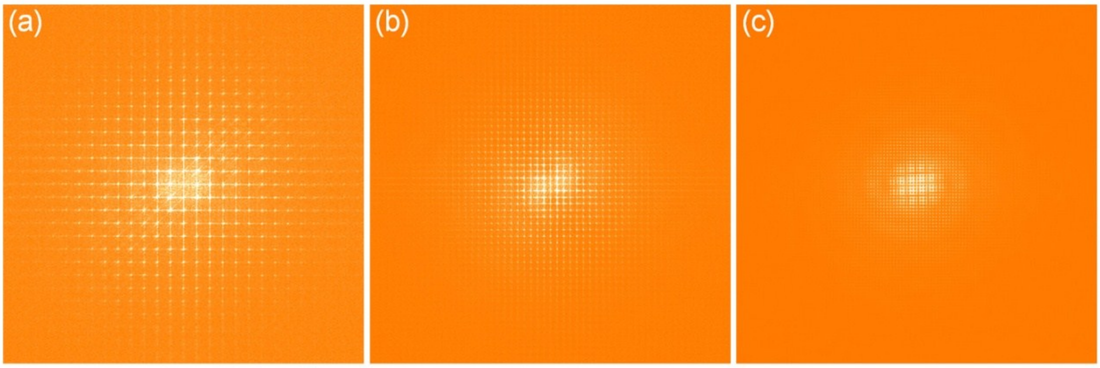

Figure S5. Two-Dimensional Fast Fourier transformation (2D-FFT) analysis for the distribution of the micropores. (a)-(c) depict the Fourier Transform profile of the SEM images in Figure 2(b). It can be seen that the frequency spectrum is distributed into ring and the radius of the ring is diffuse within a small range. This illustrates that the micropores are formed with characteristic periodic distribution in all directions.

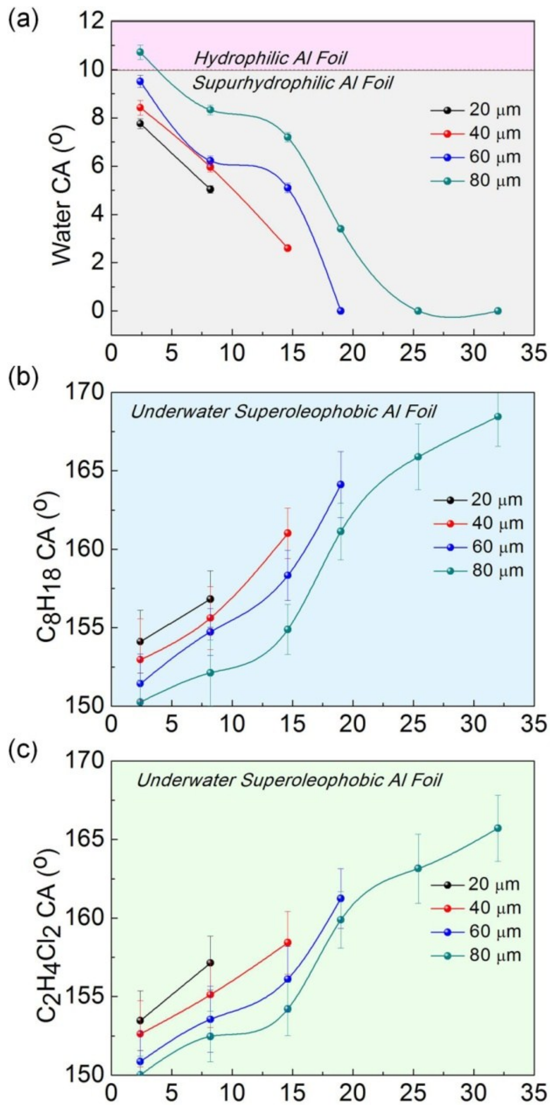

Figure S6. Systematic study of the wettability of the micropore arrays. (a) is the water contact angle on micropores with different diameters and intervals. It is indicated that most of the contact angles are less than 10°, showing superhydrophilic nature. In addition, the contact angles are decreased with the increasing micropore diameters and decreasing intervals. (b) and (c) are the C_8H_{18} and $C_2H_4Cl_2$ contact angles on micropore arrays. It can be seen that all the contact angles are larger than 150°, exhibiting underwater superoleophobic property. From (b) and (c), it is observed that the oil contact angles are increased with the increasing micropore diameters and decreasing intervals. This study illustrates that the wettability can be accurately controlled by changing the micropore diameters and intervals.

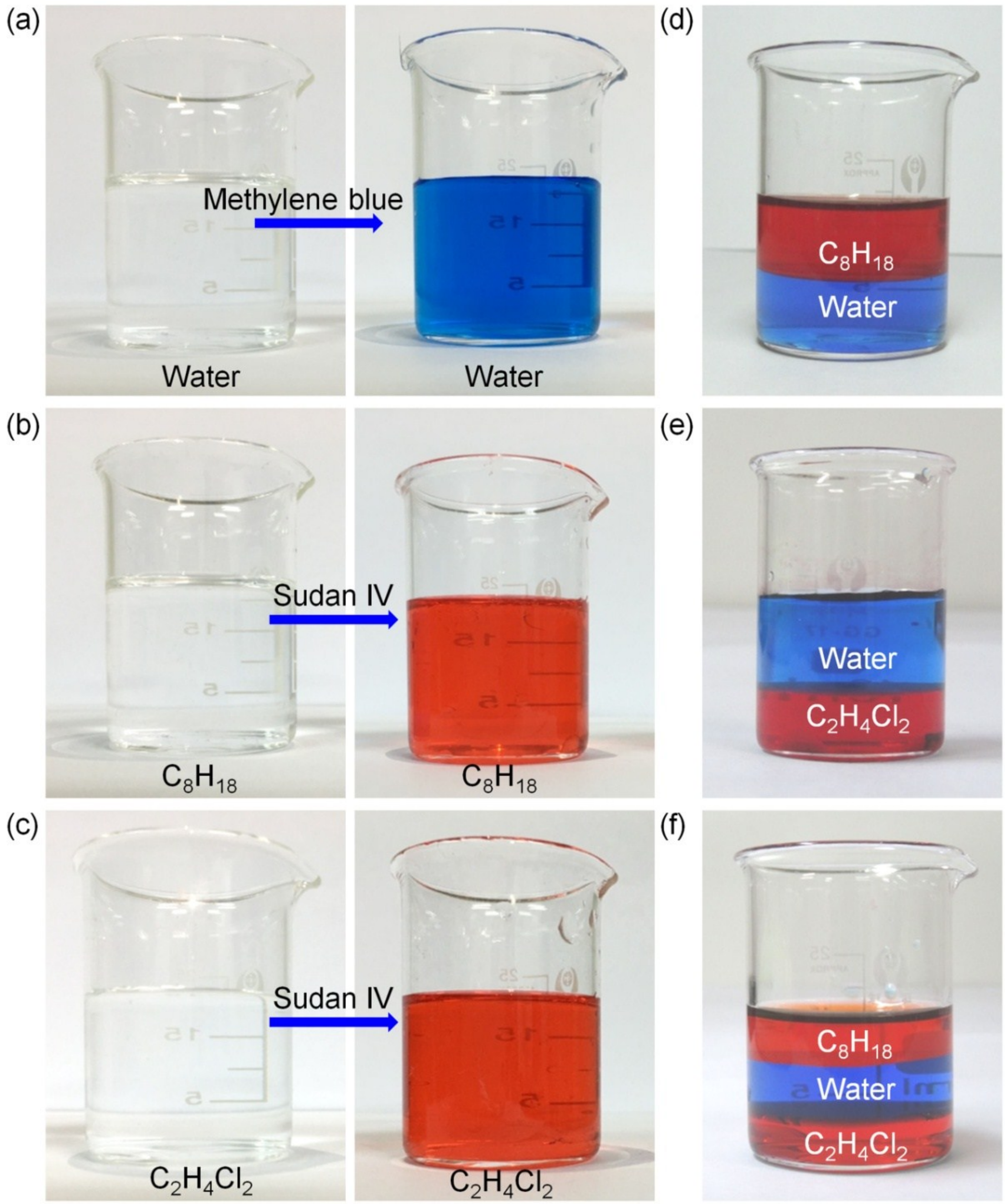

Figure S7. Preparation of the oil/water mixtures. From (a) to (c), it can be seen that the undyed water, C_8H_{18}, and $C_2H_4Cl_2$ are colorless transparent. The water presents blue color after it is dyed with methylene blue. Meanwhile, the C_8H_{18} and $C_2H_4Cl_2$ show red color after dyed with Sudan IV. It is observed from (d) to (f) that the layered oil and water is formed due to C_8H_{18} is lighter than water while $C_2H_4Cl_2$ is heavier than water.

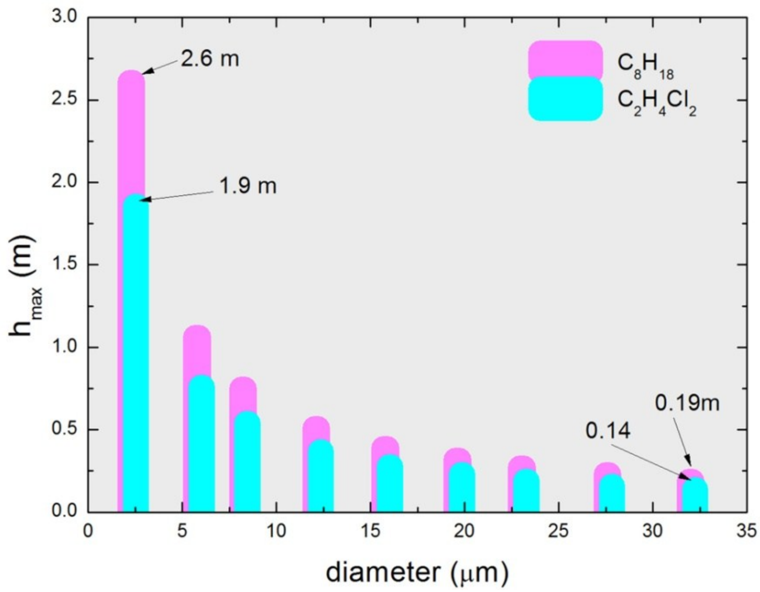

Figure S8. Calculation of the maximum height of the oil layer which can be supported by the aluminum foil. To assess the separation capability, we calculated the maximum height of the oil layer that the aluminum foil can withstand which is deduced from equations (1) and (2)

$$P_{\exp} = \rho g h_{\max} \qquad (1)$$

$$P_{theor} = 2\gamma_{OW} \cos\theta_{OW} / d \qquad (2)$$

if the P_{exp} is equal to P_{theor}, h_{max} can be expressed as

$$h_{\max} = \frac{2\gamma_{OW} \cos_{OW}}{\rho g d} \qquad (3)$$

the surface tension γ_{OW} for C_8H_{18} and $C_2H_4Cl_2$ is 21.7 and 28.1 mN/m. The oil contact angles for C_8H_{18} and $C_2H_4Cl_2$ is 10.2° and 10.9°, respectively. In addition, the density ρ for C_8H_{18} and $C_2H_4Cl_2$ are 0.70 and 1.26 g/cm^3. g is the gravitational acceleration, and the value is 9.8 N/kg. Hence, the maximum height for different diameters can be calculated, and the representative results can be seen in Figure S7.

Due to the fast and complete discharge of the water and oil from the separator (**Figure 4c**), the height of the oil layer can not exceed the critical height h_{max}.

Therefore, the oil/water separation in our experiments can not be affected by the intrusion pressure.

Supporting Information, Movie S1 The separation of light oil C_8H_{18} and water mixtures.

Supporting Information, Movie S2 The separation of heavy oil $C_2H_4Cl_2$ and water mixtures.

Supporting Information, Movie S3 The continuous oil/water separation and the recovery of the oil.